HAYATI
Journal of Biosciences

Vol. 32 No. 4, July 2025 879-895
DOI:10.4308/hjb.32.4.879-895
ISSN: 1978-3019
EISSN: 2086-4094

Research Article

Antiplasmodial Activity, Cytotoxicity, and Active Compounds Analysis of Active Fraction of *Harmsiopanax aculeatus* Leaves from Maluku, Indonesia

Rachel Turalely[1,2*], Mustofa[3], Triana Hertiani[4], Mahardika Agus Wijayanti[5]

[1]*Doctoral Program of Biotechnology, Graduate School, Universitas Gadjah Mada, Yogyakarta, Indonesia*
[2]*Chemistry Education Study Program, Faculty of Teacher Training and Education Science, Pattimura University, Ambon, Indonesia*
[3]*Department of Pharmacology and Therapy, Faculty of Medicine-Public Health and Nursing, Universitas Gadjah Mada, Yogyakarta, Indonesia*
[4]*Department of Biological Pharmacy, Faculty of Pharmacy, Universitas Gadjah Mada, Yogyakarta, Indonesia*
[5]*Department of Parasitology, Faculty of Medicine-Public Health and Nursing, Universitas Gadjah Mada, Indonesia*

ARTICLE INFO

Article history:
Received December 20, 2024
Received in revised form February 15, 2025
Accepted March 5, 2025

KEYWORDS:
Active Fraction (F7),
Analysis compounds,
H. aculeatus leaves,
In Vitro antiplasmodial activity,
In Vivo Antiplasmodial activity

ABSTRACT

The leaves of the *H. aculeatus* plant are known as a traditional antimalarial medicinal plant in Maluku. Several studies have reported on the leaf activity of this plant, but studies on *in vitro* and *in vivo* antiplasmodial activity and the compounds in the active fraction (F7) of H.aculeatus leaf have not been reported. This study aims to determine the antiplasmodial activity of the F7 of *H. aculeatus* leaves and to analyze the compounds contained therein. *In vitro*, antiplasmodial activity was tested on *Plasmodium falciparum* strain FCR3 using a microscopic method. A cytotoxicity test was performed on Vero cells using an MTT assay. *In vivo*, the antiplasmodial activity of F7 was carried out using the 4-day suppressive test method by treating Swiss mice infected with *P. berghei*. Analysis of the compounds in an F7 was done using spray reagent and UV Vis DAD and HPLC DAD-MS with a UV detector. The results showed that the F7 was very active in vitro (IC_{50} of 0.7 µg.ml^{-1}) and *in vivo* (ED_{50} of 2.49 mg.kg BW^{-1}.d^{-1}) also selectively (SI of 8159.94) inhibited the growth of Plasmodium. The F7 contains a group of essential oils, triterpenoids, phenolic compounds, and flavonoids after being analyzed using spray reagents. Based on the analysis results, five compounds were identified: fomoxanthone, cyclopentene, microspherone, indole 3-carbaldehyde, and naamine. In addition, seven compounds were not identified.

1. Introduction

Kapur leaf (*H. aculeatus*) has long been known empirically in the community to treat malaria in Maluku. Some scientific research on the efficacy of *H. aculeatus* leaf has been reported starting from its activity as an antiplasmodial and anticancer (Turalely *et al.* 2020a). This article is scientifically reviewed and does not contain any unscientific elements. This needs to be emphasized because, in the previous article (Turalely *et al.* 2022), five active compounds were scientifically found that were not scientifically pure but had been spiritually purified to express the glory of God). Research on *H. aculeatus* leaves from a scientific perspective has been widely reported, such as previous research (Turalely *et al.* 2011) on the antiplasmodial activity of *H. aculeatus* leaf extract *in vitro* and *in vivo*, which proved that the three extracts (methanol extract, ethyl acetate extract, and hexane extract) have antiplasmodial activity. However, the methanol extract of *H. aculeatus* leaves was more active with an IC_{50} value of 13.82 g.ml^{-1} (Turalely *et al.* 2020a), and *in vivo*, it had an ED_{50} of 16.16 mg.kg BW^{-1}.d^{-1} (Turalely *et al.* 2011). The study also explained that the methanol extract was separated using vacuum liquid chromatography (VLC) and obtained in 12 fractions.

* Corresponding Author
E-mail Address: rachelturalely.unpatti@gmail.com

Based on previous research data, several fractions have reported antiplasmodial activity *in vitro* (Turalely 2018; Turalely *et al.* 2018).

Several other fractions that have never been reported for their antiplasmodial activity *in vitro* and *in vivo* as well as their cytotoxic activity, are fractions F1, F5-F11, in addition to 4 other fractions that have been reported, namely F2-F4 and F12 (Turalely 2018; Turalely *et al.* 2018). This article will discuss the antiplasmodial and cytotoxic activities of fractions F1, F5-F11. *In vivo*, antiplasmodial activity tests were also conducted on the fraction proven to be most active in vitro. This is intended to minimize costs and the use of test animals in research. Compound analysis in active fraction proven in vivo has also been conducted using GC-MS (Turalely *et al.* 2011). Still, in this article, the compound analysis will be conducted using UV-Vis DAD and HPLC DAD-MS with a UV detector. The use of tools to analyze compounds in a natural material sample greatly affects the results for detecting a compound. This is influenced by the sensitivity of the tool that can detect volatile compounds such as GC-MS, while non-volatile compounds cannot be detected with this tool; therefore, in this study, the most active fractions proven *in vitro* and *in vivo* were analyzed using UV-Vis DAD and HPLC DAD-MS. In addition, the availability of compound databases in the tool library also affects the tool's ability to read the presence of compounds in the analyzed samples. Therefore, this is our consideration for analyzing the non-volatile active compounds in the most active fraction using UV-Vis DAD and HPLC DAD-MS in our research.

2. Materials and Methods

2.1. Ethics Information

This study complies with all research ethics, especially the antiplasmodial activity testing research protocol, and has been approved by the ethics committee board of the Faculty of Medicine, Public Health, and Nursing, Universitas Gadjah Mada, with number 3.2.01-008.2013.03.

2.2. Determination of the Kapur Plant and the Main Materials and Tools used in This Study

The determination of this Kapur plant has been previously reported under the name Harmsiopanax aculeatus, Harms (Turalely *et al.* 2011), and the last determination with the Latin name Harmsiopanax aculeatus (Blume) Warb.ex Boerl (Araliaceae, Voucher Number 1 HaA) with determination number 01409/S. Tb./IX/ 2018 (Turalely *et al.* 2020b, 2022).

2.3. Materials

The main materials used in this study were: young Kapur leaves (*H. aculeatus*), solvents: *n*-hexane, chloroform, ethyl acetate and methanol analytical grade (E-Merck), *P. falciparum* FCR3 strain ANKA, *P. berghei*, Swiss mice, Silica gel 40 Merck (37-39 mesh), silica gel 60H (1105932), RPMI, DMSO, Giemsa, Vero Cell, TLC plate GF254 (E-Merck). The main tools used in this research are Laminar Air Flow, Elisa Reader, Vacuum Liquid Chromatography (VLC) column, and UV-Vis DAD, HPLC DAD-MS with UV detector.

2.4. Fractionation of *H. aculeatus* Leaf Methanol Extract

The methanol extract of *H. aculeatus* leaves, which has antiplasmodial activity *in vitro* and *in vivo* from previous studies, was fractionated using VLC by dissolving 5 grams of the test material in the solvent and then impregnated with silica gel 40 Merck (37-39 mesh). The solvent was evaporated until the mixture became dry. The n-hexane solvent was put into the chromatographic column, then silica gel 60 H (1105932) stationary phase powder, which had been mixed with n-hexane solvent in the form of silica slurry, was inserted into the column little by a little while vacuuming until the column height was ±15 cm. Columns that have been made, left overnight. The sample powder was sprinkled over the stationary phase until smooth, and the surface of the powder was covered again with silica gel 40 Merck (37-50 mesh). Elution was carried out in a gradient manner, starting with *n*-hexane, *n*-hexane-chloroform in various ratios, followed by chloroform-ethyl acetate, ethyl acetate-methanol in various ratios, and finally methanol in the obtained fractions, the solvent was evaporated and the TLC profile is seen. Fractions with similar TLC profiles were combined.

2.5. *In Vitro* Antiplasmodial Activity Assay of *H. aculeatus* Leaf Fraction

Cultures of *P. falciparum* chloroquine-resistant strain (FCR3) were modified by the candle jar method (Trager & Jensen 1976). Parasite-infected red blood cells were cultured in a culture flask containing 8 ml of complete medium (containing 10% serum), with a final hematocrit of 1.5%. The culture manipulation was in a laminar flow cabinet under aseptic conditions, then incubated in a CO_2 incubator at a temperature of 37°C.

The medium was replaced with a new one every 24 hours of the incubation period. Suppose the parasitemia is too high (more than 10%). In that case, a subculture is made by adding normal red blood cells so that the parasitemia becomes low (less than 1%) and is ready for antiplasmodial activity testing.

Each fraction obtained from the separation of the methanol extract weighed ±2 mg dissolved with 100 µL (less than 5%) DMSO, then added RPMI to a volume of 2 ml as a stock solution with a concentration of 1,000 $g.ml^{-1}$. The stock solution was diluted with RPMI, and then a concentration series was made. The concentration series for the combined fractions (F) 1, 2, 3, 4, 5, 6, 8, 9, 10, 11, and 12 are 400, 200, 50, 25, 5, and 1 $\mu g.ml^{-1}$. At the same time, the concentration series for F7 is 30, 25, 12.5, 10, 5, 2.5, 0.5, 0.25 and 0.125 $\mu g.ml^{-1}$. Each concentration was made triplet.

The parasite used for the antiplasmodial test is the ring stage. How to get it is by synchronization with a 5% sorbitol solution. After synchronization, parasite microculture was made. The microplate used had 96 wells for the control and treatment groups. The final volume of suspension for control and treatment in each well was prepared as much as 100 µL of complete medium containing parasites with 3% hematocrit and 2% parasitemia. Then, 100 µL of the test material or complete medium was added to the parasite so that a culture with a final hematocrit of 1.5% and parasitemia of 1% was added. Each extract has been made in a series of different concentrations and made triplets. The microplate was then placed in a vacuum desiccator box using a candle jar and then incubated in a CO_2 incubator at 37°C for 72 hours. After the incubation period ended, each sample was smeared and stained with Giemsa dye for further parasitemia, which was visually calculated with a microscope. In this procedure, extracts and fractions were carried out to confirm previous research data, as well as one of the steps in the process of characterizing the antiplasmodial active compound in *H. aculeatus* leaves.

2.6. Cytotoxicity Activity Test of *H. aculeatus* Leaf Active Fraction against Vero Cells

Inactivated Vero cells in ampoule containers (cryo tube) were taken from the liquid nitrogen tank or the -80°C freezer and immediately thawed at room temperature until just melted. The ampoules were sprayed with 70% alcohol. The ampoule was opened, and the cell suspension was transferred dropwise into a sterile conical tube containing a culture medium (CM) with a 1,000 L micropipette. The cell suspension was centrifuged at 6,000 rpm for 5 minutes, then the supernatant was discarded. The culture medium used for the cytotoxicity test on Vero cells used M199 media. Then, 4 ml of M199 media (Vero cells) were added and resuspended slowly until homogeneous using a pipette. Next, 2 ml of cell suspension was grown in several tissue culture dishes (2-3 pieces), added with 5 ml of CM each in a tissue culture dish, and homogenized. Cells were observed under a microscope and incubated in an incubator at 37°C with a flow of 5% CO_2. After reaching the incubation period of 24 hours, the medium was changed, and cells were grown again until they were confluent and sufficient in number for the study. After a sufficient number of cells (80% confluent), the medium was removed by micropipette or Pasteur pipette. Colonies were washed with PBS two times. Then trypsin-EDTA (trypsin 0.25%) was added evenly and incubated in the incubator for 3 minutes. Then, 5 ml of new CM was added to inactivate trypsin. Cells were resuspended in the medium and then transferred into a sterile conical tube. After that, cells were counted using a hemocytometer. The cells to be planted on the plate were transferred to the required number of cells and placed into a new conical tube, and CM was added according to the desired concentration. A total of 5 mg of the test material was tested for solubility in DMSO. Then, 50 µL DMSO was added and dissolved with the help of a vortex. If it is not dissolved, add another 50 µL of DMSO and dissolve with the help of a vortex.

Furthermore, variations in sample concentration were made by diluting the sample in DMSO using CM. The concentration series of fractions used in the Vero cell test was 2,000, 1,000, and 500 $\mu g.ml^{-1}$. In determining the toxicity of the test material, cells were put into 96-well microplates with a density of 2×10^4 cells/well, 100 µL cells each. The condition of the cells after being treated with the test material, then the cells was observed under a microscope. Cells were incubated in an incubator for 24 hours. At the end of incubation, the culture medium containing the samples was discarded and washed with 100 µL of PBS. In each well, 100 µL of CM containing samples with various concentrations was added and incubated for another 48 hours. At the end of incubation, the culture medium containing the samples was discarded and washed with 100 µL of PBS. Then 100 µL of culture medium was added to each well containing 5 µg.mL-1 of MTT tetrazolium salt (3-(4,5-dimethylthiazole-2-il)-2,5-diphenyltetrazolium bromide) and incubated again for 4 hours at 37°C. Live cells will react with MTT

to purple formazan. After 4 hours, 100 µL SDS 10% stopper reagent was added to each well in 0.1 N HCl to kill cells and dissolve formazan crystals. The plate was wrapped in aluminum foil and then incubated at room temperature in the dark for one night. Furthermore, the absorbance of each well was read with an ELISA reader at a wavelength of 595 nm. In this procedure, extracts and fractions are carried out to confirm the data of previous studies that have been carried out.

2.7. *In Vivo* Antiplasmodial Activity Test Active Fraction of *H. aculeatus* Leaves

The *in vivo* antiplasmodial activity test of the most active fraction of *H. aculeatus* leaves was carried out using the four-day suppressive test method with the procedure carried out in previous studies (Turalely *et al.* 2011). The dose of active fraction of *H. aculeatus* leaf used in this research was 0.625, 1.25, 2.5, 5, and 10 mg.kg $BW^{-1}.d^{-1}$. The positive control used was a single dose of chloroquine, which was 0.927 mg.kg $BW^{-1}.d^{-1}$.

2.8. Analysis of Compound Components in the Active Fraction of *H. aculeatus* Leaves

The most active fraction (FA) obtained in this study is the combined fraction seven (F7) which is the dissolved fraction in chloroform-ethyl acetate (8:2). This fraction was then analyzed for phytochemical using TLC and Lieberman-Burchard, $FeCl_3$, and Anisaldehyde sulfate sprays reagent. In addition, F7 was analyzed using UV-Vis DAD and HPLC DAD-MS with a UV detector. The data from this study were analyzed qualitatively for both phytochemical analysis (compound groups) using spray reagents and analysis of compounds identified based on UV-Vis DAD and HPLC DAD-MS results with a UV detector.

3. Results

3.1. Fractionation of *H. aculeatus* Leaf Methanol Extract

The fractionation of the methanol extract of the leaves of *H. aculeatus* obtained 16 fractions, and after monitoring using TLC, the same profiles were combined. Hence, the fraction obtained from this fractionation was 12. The TLC profiles can be seen in Table 1 and Figures 1, 2, and 3.

3.2. Antiplasmodial Activity *In Vitro* Leaf Fraction of *H. aculeatus*

The results of the *in vitro* antiplasmodial activity of the leaf fraction of *H. aculeatus*, as described previously, have been reported in previous studies, but some fractions have not been reported. The test result data can be seen in Tables 2, 3, and 4.

Based on the *in vitro* antiplasmodial activity test data on 12 fractions of the methanol extract of *H. aculeatus* leaves, 11 fractions were tested in this study, namely the F2-F12 fraction. The results of this study showed that of the 11 fractions tested, two fractions had high antiplasmodial activity, namely F5 and F7, as shown in Tables 5 and 6. Six fractions were categorized as having moderate activity, namely F2, F3, F4, F6, F9, and F12. The other two fractions were categorized as having moderate activity, namely F8 and F11. In addition, two other fractions were categorized as inactive, namely F1 and F10. Among the 12 fractions, the most active fraction was F7, and the least active fraction was F1. The F7 fraction, which is the most active fraction (FA), has an IC_{50} of 0.7 µg.mL^{-1} (Table 3).

3.3. Cytotoxicity Activity of *H. aculeatus* Leaf Fraction against Vero Cells

The results of the cytotoxicity activity of the fraction of *H. aculeatus* leaf against Vero cells have been carried out, and several fractions have been reported in

Table 1. The mobile phase used in VLC and the number of fractions obtained after monitoring using TLC

Eluent	Ratio of eluent v/va	Volume (ml)	Fraction
n-hexane	100%	500	1
n-hexane: chloroform	70:30	300	2
n-hexane: choroform	50:50	200	3
n-hexane: chloroform	30:70	200	4
Chloroform	100%	300	5
Chloroform: ethyl acetate	90:10	200	6
Chloroform: ethyl acetate	80:20	200	7
Chloroform: ethyl acetate	70:30	200	
Chloroform: ethyl acetate	60:40	200	8
Chloroform: ethyl acetate	50:50	200	
Chloroform: ethyl acetate	20:80	200	9
Ethyl acetate	100%	200	
Ethyl acetate: methanol	70:30	200	10
Ethyl acetate: methanol	50:50	200	11
Ethyl acetate: methanol	30:70	200	12
Methanol	100%	400	

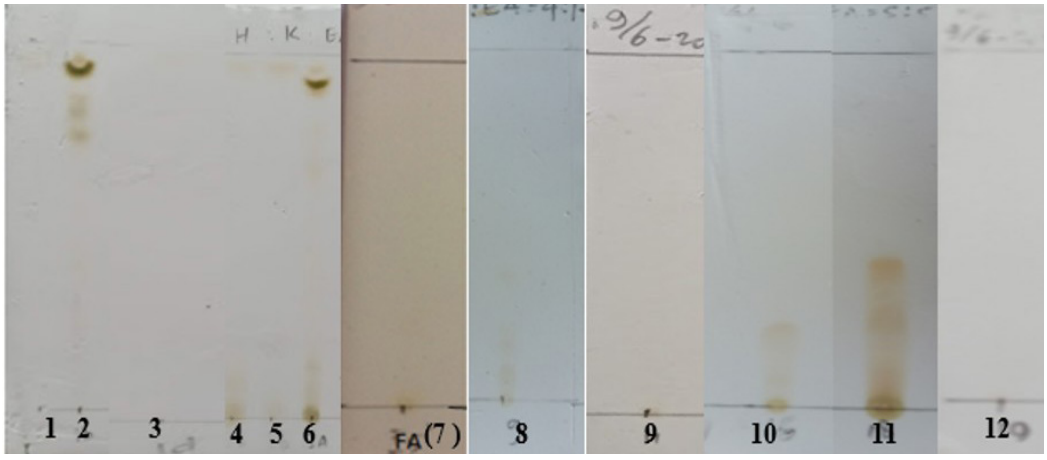

Figure 1. Profile of the 12 fractions of *H. aculeatus* leaf in visible light. Fractions 1-6 using mobile phase hexane: chloroform: ethyl acetate 2:7:1, stationary phase: silica gel GF254. Fractions 7-9 used chloroform: ethyl acetate 4:1 as the mobile phase, stationary phase: silica gel GF254, fractions 10-11 used chloroform: ethyl acetate as mobile phase 5:5, stationary phase: silica gel GF254, fraction 12 used chloroform: ethyl acetate 4:1 as the mobile phase, stationary phase: silica gel GF254

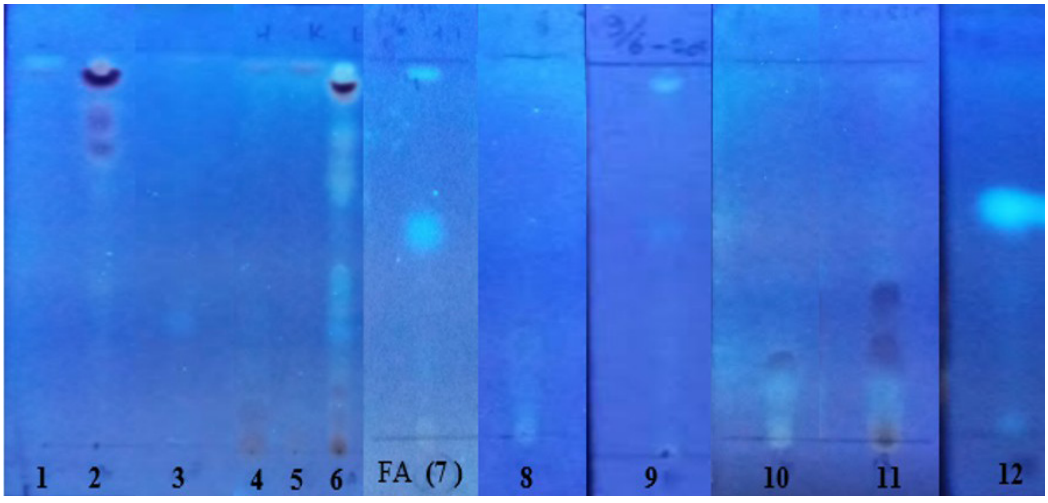

Figure 2. TLC profile of 12 fractions of *H. aculeatus* leaf at UV 366 nm

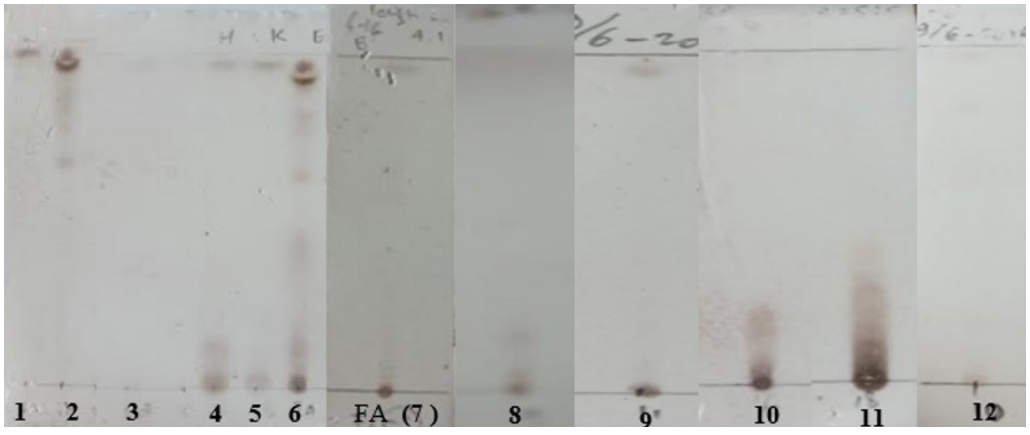

Figure 3. TLC profile of 12 fractions of *H. aculeatus* leaf after spraying with Cerium (IV) sulfate

previous studies, but some have not been reported. The data from the selectivity index cytotoxicity test for 12 leaf fractions of *H. aculeatus* can be seen in Table 5.

Based on data from the cytotoxicity test and selectivity index of the 12 fractions, nine selective fractions inhibited Plasmodium growth, while three non-selective fractions inhibited Plasmodium growth. The value of the selectivity index of F7 in the data shows that it is larger compared to the other 11 fractions, so it is very selective in inhibiting the growth of Plasmodium.

Table 3. *In vitro* antiplasmodial activity of F7 leaves *H. aculeatus* against *P. falciparum* strain FCR3

Concentration (µg.ml^{-1})	Parasitemia inhibition (%)	IC_{50} (µg.ml^{-1})
0.125	38.80 ± 3.21	
0.25	47.96 ± 4.60	
0.5	51.71 ± 4.10	
2.5	52.31 ± 8.82	
5	54.61 ± 8.33	0.7
10	61.63 ± 7.01	
12.5	67.29 ± 6.72	
25	71.24 ± 6.51	
30	79.81 ± 3.66	

Table 2. *In vitro* antiplasmodial activity of F1-F7 leaves *H. aculeatus* against *P. falciparum* strain FCR3

Concentration (µg.ml^{-1})	Parasitemia inhibition (%)					
	F1	F2*	F3*	F4*	F5	F6
1	2.36±0.77	41±1.31	34.7±0.47	43.86±0.86	30.54±1.05	39.44±2.54
5	9.61±2.60	42.56±1.33	40.33±0.19	47.95±0.55	62.51±1.06	48.21±5.52
25	15.27±3.07	51.07±1.06	51.33±1.30	51.40±0.82	71.41±0.99	69.53±0.52
50	28.00±2.36	56.79±0.15	64.07±0.92	56.27±1.56	90.44±0.94	70.76±2.59
200	55.68±2.69	87.85±1.04	92.2±1.53	66.47±2.10	94.35±0.98	94.41±1.96
400	69.85±1.35	89.67±0.72	94.47±1.16	81.61±0.79	94.61±1.25	96.56±0.74
IC_{50} (µg.ml^{-1})	153.85	7.48	8.24	7.75	3.24	5.63

*published (Turalely *et al.* 2018)

Table 4. Antiplasmodial activity *in vitro* of fraction 8-12 of *H. aculeatus* leaf against *P. falciparum* strain FCR3

Concentration (µg.ml^{-1})	Parasitemia inhibition (%)				
	F8	F9	F10	F11	F12**
1	18.00 ±2.01	30.41±2.43	22.29±2.06	32.10±2.04	43.86±2.88
5	26.38 ± 3.98	44.31±1.64	27.22±4.48	39.89±1.02	47.95±3.98
25	40.74 ± 1.09	47.95±3.59	13.97±2.63	47.12±1.07	51.40±1.93
50	47.11 ± 3.92	66.8±4.68	36.13±2.02	47.56±1.23	56.27±1.50
200	74.59 ± 1.87	75.40±4.13	54.71±1.58	60.33±3.00	66.47±2.55
400	90.44±3.94	85.29±4.26	70.31±2.46	71.09±1.04	81.61±2.10
IC_{50} (µg.ml^{-1})	30.97	11.54	108.41	39.42	7.75

**data has been published (Turalely 2018)

Table 5. Vero cells IC_{50} data and selectivity index of *H. aculeatus* leaf fraction

Fraction	IC_{50} *P. falciparum*	IC_{50} vero cells (µg.ml^{-1})	Selectivity index (SI)	Category
F1	153.85	519.78	3.38	Not selective
F2*	7.48	5814.43	777.33	Selective
F3*	8,24	7780.48	944.23	Selective
F4*	7.75	1022.44	131.93	Selective
F5	3.24	1064.07	328.42	Selective
F6	5.63	2242.49	398.31	Selective
F7	0.7	5548.76	8159.94	Selective
F8	30.97	677.56	21.88	Not selective
F9	11.54	6516.39	564.68	Selective
F10	108.41	9863.16	90.98	Selective
F11	39.42	0	0	Not selective
F12**	7.75	4945.45	638.12	Selective

*published (Turalely *et al.* 2018), **published (Turalely 2018)

3.4. *In Vivo* Antiplasmodial Activity of Active Fraction of *H. aculeatus* Leaves

The results of the *in vivo* antiplasmodial activity test of the active fraction (F7) of *H. aculeatus* leaves infected with *P. berghei* in Swiss mice showed F7 activity, which was very active in inhibiting Plasmodium growth with an ED_{50} value of 2.49 mg.kg $BW^{-1}.d^{-1}$. The results of the *in vivo* antiplasmodial activity test data on the active fraction of *H. aculeatus* leaves can be seen in Table 6.

3.5. Analysis of Compound Components in the Active Fraction of *H. aculeatus* Leaves

The active fraction (F7) of *H. aculeatus* leaves, which had proven activity as antiplasmodial both *in vitro* and *in vivo*, was then monitored using TLC in visible light, as well as UV 254 nm and 366 nm. Furthermore, the obtained TLC profile was screened for phytochemicals using spray reagents. The TLC profile data can be seen in Figure 4 and Table 7, while the phytochemical screening of the active fraction (F7) can be seen in Table 8.

The active fraction (F7) was further analyzed to determine the components of the compounds using UV-Vis DAD. The results showed that there were 12 listed on the chromatogram, but only five compounds were identified, as shown in Table 9 and 10. In comparison, the other seven compounds were unknown (temporary suspicions were new compounds) and could be identified when characterizing the active compounds after elucidating their structure.

The data obtained in Table 9 are the results of molecular weight analysis of compounds using the LC-MS tool, which were analyzed at the Institute of Pharmaceutical Biology and Biotechnology, Heinrich Heine University, Duesseldorf. However, after analyzing the molecular weights recorded on the HPLC DAD-MS with UV detector tool, none of them matched the molecular weights of the five compounds identified with UV-Vis DAD. This shows that the identified molecular weights are not derived from the five compounds identified.

Table 6. *In vivo* antiplasmodial activity of fraction 7 (F7) against *P. berghei* infected in Swiss mice

Dose (mg. kg BW^{-1}. d^{-1})	Parasitemia ± SD	Inhibition (%) ± SD	ED_{50} (mg. kg BW^{-1})
10.625	3.50±1.82	25.46±12.79	
1.25	2.89±1.76	38.58±20.66	
2.5	1.99±0.90	57.59±8.98	
5	1.81±1.68	61.42±12.69	2.49
10	1.52±1.31	67.70±23.04	
0*	4.70±0.78	0.00±0.00	
0.927**	2.16±1.36	83.44±10.64	

#Negatif control (without giving F7), **Positive control (Chloroquin); SD: standard deviation

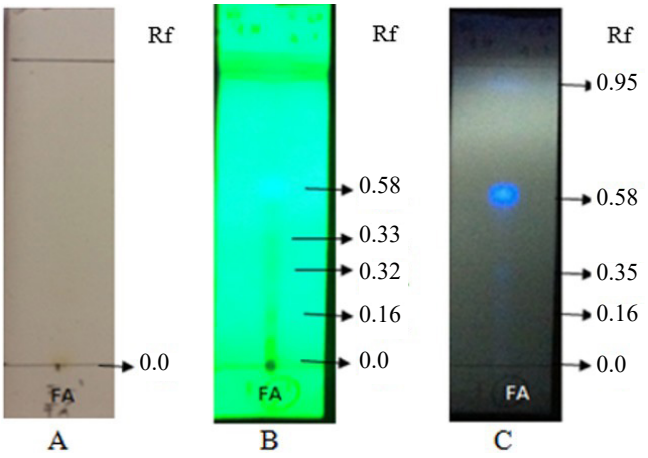

Figure 4. The FA (F7) Chromatogram using the TLC figure is too small. (A) F7 in visible light, (B) F7 at UV 254 nm, (C) F7 at 366 nm, UV. Mobile phase: chloroform: ethyl acetate (4:1) Stationary phase: Silica gel 60 GF254

Table 8. Screening phytochemical active fraction (F7) using spray reagent

Spray reagent	Observation	Interpretation
Anisaldehyde sulfate*	Reddish yellow spot	Essential oil (+)
Lieberman-Burchard*	Brownish-yellow	Triterpenoid (+)
$FeCl_3$**	Yellow spot	Phenolic compounds, flavonoids(+)

Table 7. Interpretation of F7 chromatogram

Chromatogram A visible light			Chromatogram B (λ = 264 nm)			Chromatogram C (λ = 366 nm)		
Spot	Color	Rf	Spot	Color	Rf	Spot	Color	Rf
1	Light brown	0.0	1	Light blue fluorescence	0.58	1	Light blue fluorescence	0.95
			2	Light brown	0.33	2	Dark blue fluorescence	0.58
			3	Light brown	0.32	3	Light blue fluorescence	0.32
			3	Light brown	0.16	3	Light blue fluorescence	0.16
			5	Brown	0.0	5	Yellow fluorescence	0.0

Table 9. UV-Vis DAD data of active fraction of *H. aculeatus* leaves

λ = 235 nm		λ = 254 nm		λ = 280 nm		λ = 280 nm	
tR (minutes)	Type of compounds	tR (minutes)	Type of compounds	tR (minutes)	Type of compounds	tR (minutes)	Type of compounds
7.670	Phomoxanthone	12.68	Nf	13.657	Nf	17.5	Nf
12.673	Cyclopenin	13.647	Nf	14.17	Nf	17.63	Nf
13.660	Nf	16.03	Nf	16.06	Nf	24.02	Nf
15.567	Nf	17.167	Nf	17.173	Nf	26.06	Nf
17.177	Nf	17.633	Nf	17.63	Nf		
17.617	Microsphaerone	18.107	Nf	18.09	Nf		
18.097	Indole-3-carbaldehyde	24.627	Nf	13.657	Nf		
21.650	Nf	12.68	Nf				
36.047	Naamine						
48.640	Nf						
49.407	Nf						
57.270	Nf						

This database was obtained from the Institute of Pharmaceutical Biology and Biotechnology, Heinrich Heine University, Duesseldorf, where samples were analyzed using a UV-Vis DAD. Nf = Not found

Table 10. Active fraction (F7) LC-MS data

ESI^+		ESI^-	
tR (minutes)	Pseudo molecular ion peak	tR (minutes)	Pseudo molecular ion peak
19.52	783.3	19.66	942.1
23.7	954.4	23.75	851.8
24.23	992	24.38	794.2

4. Discussion

4.1. *In Vitro* Antiplasmodial Activity and Cytotoxicity on Vero Cells of Fraction of *H. aculeatus* Leaf

Based on the *in vitro* activity test results of the 12 fractions obtained from the separation of methanol extract from *H. aculeatus*, nine fractions selectively inhibited Plasmodium growth, and three non-selective fractions inhibited Plasmodium growth. This research also shows that six fractions are categorized as having moderate activity, namely F2, F3, F4, F6, F9, and F12. The other two fractions were categorized as having moderate activity, namely F8 and F11. In addition, two other fractions were categorized as inactive, namely F1 and F10. Among the 12 fractions, the most active fraction was F7, and the least active fraction was F1. The F7 fraction, which is the most active fraction (FA), has an IC_{50} of 0.7 $\mu g.ml^{-1}$ (Table 3). Fraction 1, which is inactive at this stage of *in vitro* activity testing, does not mean it is not active. This was proven after further analysis at the isolation stage of the active compound, and it turned out that F1 had high antiplasmodial activity. This is because there are still many dominant compounds that do not have antiplasmodial activity in F1, so the F1 activity is the least active among the 11 other fractions, as described in the study of (Turalely *et al.* 2022).

The composition of the dominant compound present in each fraction also influenced the difference in the antiplasmodial IC_{50} value of the 12 fractions. Fractions F7, F9, and F12 have similar spot patterns. Qualitatively, it can be said that F7, F9, and F12 have the same dominant compound. However, F9 has a smaller antiplasmodium activity, as evidenced by a larger IC_{50} value, compared to F7 and F12, which have the same IC_{50}. Based on the TLC spot pattern at UV 366 nm (Figure 2), it is obvious that the spot of this dominant compound in F12 is larger than in F7 and appears the faintest in F9. Evidence from this spot data can be explained that this dominant compound is more polar. In F7, this spot is more visible than in F9. This can be caused by the fact that in F9, there is another compound that is more dominant with almost similar polarity but is not/less active in inhibiting the growth of *Plasmodium falciparum*. Hence, the ability to kill *Plasmodium falciparum* is smaller (large IC_{50} value). This is in contrast to F7, which has greater antiplasmodium activity with a smaller IC_{50} value, compared to F12, which has the same spot pattern (Figure 2). Both fractions have the same spot pattern, which is very visible in UV light at 366 nm. However, in addition to F7 having a dominant active compound that appears like spot F9 or F12, F7 also has other active compound spots that support each other's ability to kill *Plasmodium falciparum*, so that F7 has much greater antiplasmodium activity than F12 or F9. Therefore, based on the results of the antiplasmodium activity test on *Plasmodium falciparum*, the ability of fractions F2-F7 and F12 to kill *Plasmodium falciparum* is much greater compared to other fractions, as evidenced by the smaller IC_{50} value. Overall, of the 12 fractions of the methanol extract, fraction F7 was shown to have a much greater activity to inhibit the growth/kill of *Plasmodium falciparum*.

The TLC profiles in Figures 1, 2, and 3 show that F1 has a different spot pattern than F2-F7. In the F2-F7 fraction, several dominant compounds at 366 nm UV are similar, causing the antiplasmodial activity of F2-F7 to have a large difference in IC_{50} value. Likewise, the TLC profiles of F8 and F9 are similar so that their antiplasmodial activity is not too large. In the TLC profile, F10 is similar to F11, but its activity is very different. It is strongly suspected that one spot on F11 that F10 does not have has a strong enough influence in inhibiting the growth of *P. falciparum* so that it also affects the IC_{50} value of F11, which is smaller than F10. At F12, antiplasmodial activity was very different from F10 and F11. This is reinforced by the presence of the TLC profile of the F12, which is very different from the F10 and F11. This difference can be caused by differences in the composition of the dominant compound contained in F12.

The difference in antiplasmodial IC_{50} values in the 12 fractions is also influenced by the composition of the dominant compounds found in each fraction. The TLC profiles show that F1 has a different spot pattern from F2-F7 (Figures 1, 2, and 3). In fractions F2-F7, there are the same TLC spots, which qualitatively indicate that the dominant compounds are the same/have the same polarity so that they are in the same spot position. This is what causes the antiplasmodial activity of F2-F7 to be greater and has a fairly large difference in IC_{50} values with other fractions. Likewise, the TLC profiles of F8 and F9 are similar so that their antiplasmodial activity is not too large. In the TLC profile, F10 is similar to F11, but its activity is very different. It is strongly suspected that one of the spots in F11 that F10 does not have has a fairly strong influence in inhibiting the growth of *P. falciparum*, so it also affects the IC_{50} value of F11, which is smaller than F10. In F12, antiplasmodial activity is very different from F10 and F11. This is reinforced by the presence of a TLC profile of F12, which is very different from F10 and F11. This difference can be caused by differences in the composition of dominant compounds found in F12. The difference in antiplasmodial IC_{50} values from the 12 fractions is also influenced by the composition of dominant compounds found in each fraction. The TLC profiles show that fraction 1 (F1) has a different spot pattern from F2-F7. In fractions F2-F7, there are several dominant compounds at a similar UV wavelength of 366 nm, causing the antiplasmodial activity of F2-F7 to have a large difference in IC_{50} values (Figures 1, 2, and 3). Likewise, the TLC profiles of F8 and F9 are similar so that their antiplasmodial activity is not too large. In the TLC profile, F10 is similar to F11, but its activity is very different. It is strongly suspected that one of the spots on F11 that F10 does not have has a strong enough effect in inhibiting the growth of *P. falciparum*, so it also affects the IC_{50} value of F11, which is smaller than F10. In F12, antiplasmodial activity is very different from F10 and F11. This is reinforced by the presence of a TLC profile of F12, which is very different from F10 and F11. This difference can be caused by differences in the composition of the dominant compounds contained in F12.

4.2. *In Vivo* Antiplasmodial Activity Active Fraction (F7) of *H. aculeatus* Leaves

The data from the in vivo antiplasmodial test on the active fraction (F7) of *H. aculeatus* leaves, as shown in Table 5, prove that F7 is very active in inhibiting the growth of Plasmodium. Based on previous research (Muñoz *et al.* 2000), the *in vivo* antiplasmodial activity of the test material is categorized as very active if it has an ED50 of 100 mg.kg $BW^{-1}.d^{-1}$. Thus, this fraction's *in vivo* antiplasmodial activity is also categorized as very active compared to the methanol extract in previous research (Turalely *et al.* 2011). This fraction has higher antiplasmodial activity *in vivo*, and compared with the positive control (chloroquine), the antiplasmodial activity of F7 is smaller. This indication shows that chloroquine has better antiplasmodial activity. However, this comparison cannot be used comprehensively because F7 is not a pure compound like chloroquine. However, the composition of other compounds in F7 also affects the activity of F7 in inhibiting Plasmodium.

When compared to the methanol extract of *H. aculeatus* leaves, F7 has greater antiplasmodial activity. This proves that the methanol extract is still mixed with other compounds that do not have antiplasmodial activity. Therefore, its activity is much smaller compared to its active fraction (F7). The inhibitory activity of *P. berghei* for four days also shows that for all doses tested, it turns out that on the second day, there was a decrease in inhibition of *P. berghei* growth. The decrease due to the response of the mice's body to the administration of the test material (F7) was not optimal. However, from the third to the fourth day, the inhibition of *P. berghei* growth increased, as shown in Figure 5.

The data on the inhibitory profile of parasitemia in Swiss mice infected with *P. berghei* after being treated with the active fraction (F7) strengthens the potential of F7 as an antiplasmodial.

The data from this research are in line with the research conducted by (Turalely *et al.* 2011). Erythrocytes infected with *P. berghei* in this study can be seen in Figure 6.

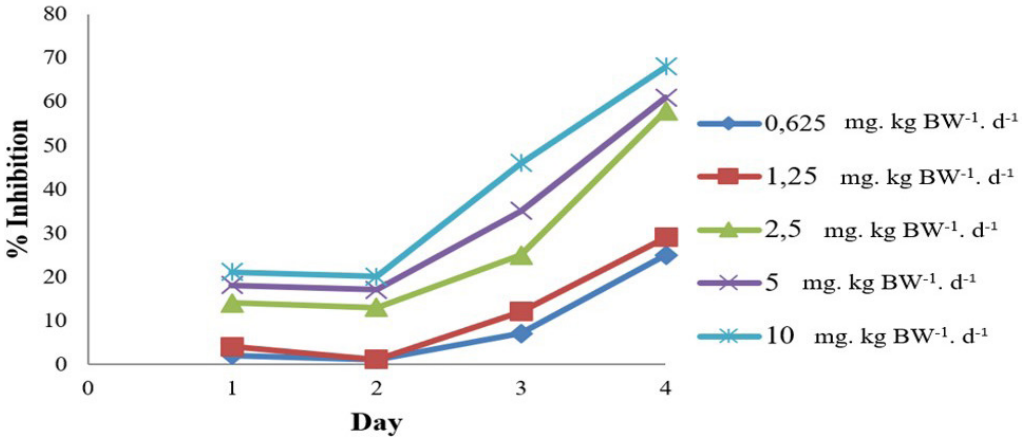

Figure 5. Profile of parasitemia inhibition in Swiss mice infected with *P. berghei* after treatment with F7

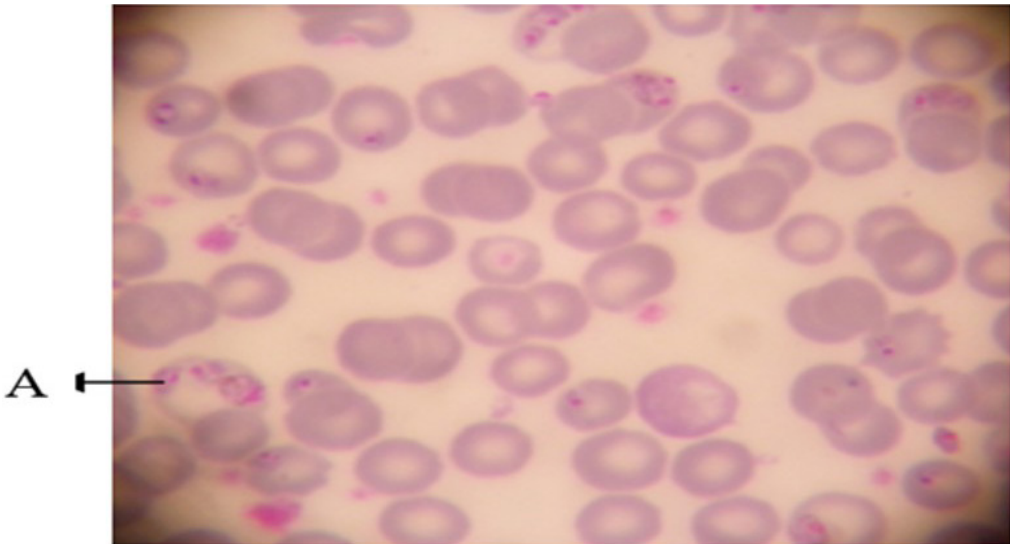

Figure 6. Overview of Swiss mice erythrocytes infected with *P. berghei*

Plasmodium berghei is a hemoprotozoa that causes malaria in rodents, especially small rodents. *Plasmodium berghei* was chosen in this study because *P. berghei* is widely used in research on the biological development of malaria parasites in humans and the availability of *in vitro* culture and purification technology at the stages of its life cycle, knowledge of genome composition, and its regulation. In molecular analysis, *P. berghei* is the same as Plasmodium, which infects humans, especially *P. falciparum*, with the same level of virulence (Darlina *et al.* 2016). Based on data on antiplasmodial activity *in vitro, in vivo*, and cytotoxic activity in Vero cells, this fraction has the potential to be developed for further research to find new antiplasmodial compounds because it can inhibit the growth/kill Plasmodium that infects erythrocyte cells in rodents, in this case, Swiss mice used as model animals/test animals and even humans.

4.3. Analysis of Compound in the Active Fraction (F7)

Analysis of active compound components in the active fraction (F7) using UV-Vis DAD obtained five compounds. Several compounds were identified in the UV-Vis DAD data (Table 9) through the results of phytochemical tests (Tables 7 and 8). The data in Table 10 show that F7 still contains many compounds. This is evidenced by the detection of 13 compounds at a wavelength of 235 nm, six of which, after being confirmed by the database, were identified as phomoxanthone, cyclopenin, microsphaerone, indole-3-carbaldehyde, and naamine. Eight compounds were detected at 254 nm, seven compounds were detected at 280 nm, and four compounds were detected at 340 nm.

Phomoxanthone A and other phomoxanthone derivatives are secondary metabolites typical of the fungal genus

Phomopsis. Phomoxanthone is a group of xanthones, which are simple tricyclic scaffolding compounds that are mostly found as secondary metabolites in higher plants and microorganisms. Xanthones have a very diverse biological profile, including antihypertensive, antioxidant, antithrombotic, and anticancer activities, depending on various structural properties and different substitution positions. Chemically, Phomoxanthone is a homodimer of two tetrahydroxanthones with two units covalently linked by biaryl bonds with four hydroxyl groups replaced by acetyl groups and four free alcohol (phenolic) functions. The binding site between the two dimeric subunits is the only structural difference between Phomoxanthone A and its less toxic isomers, Phomoxanthone B and dicerandrol C. In Phomoxanthone A, the two xanthoneoid monomers are linked symmetrically at the C-4,4′ position, while Phomoxanthone B is structurally nearly identical but is linked asymmetrically at C-2,4′. Phomoxanthone A is unstable in polar solvents for a moderate time, with the covalent bond between the two monomers shifting between 2,2′-, 2,4′-, and 4,4′- bonds. More interestingly, Phomoxanthone A was first identified as an antimalarial compound, showing potent antibiotic activity against the protozoan parasite *Plasmodium falciparum*, then against Mycobacterium tuberculosis and human cancer cells (Böhler *et al.* 2018). In testing Phomoxanthone A on human cancer cells, Phomoxanthone initially showed significant pro-apoptotic properties. Phomoxanthone A is not toxic to normal healthy cells. However, it can be an activator of natural killer cells, namely murine T lymphocytes and macrophages that encode immune system stimulation along with its pro-apoptotic activity, thus working more effectively and can help in counteracting the phenomenon of resistance during chemotherapy (Yang *et al.* 2020). Phomoxanthone A also exerts bacteriostatic effects against *Bacillus subtilis, Escherichia coli, Staphylococcus aureus, Salmonella typhimurium*, and *Pseudomonas aeruginosa* (Ramos *et al.* 2022).

Eight Phomoxanthones have been isolated in the last 10 years. Two of them have been identified, and the first to be isolated were Phomoxanthone A and Phomoxanthone B from the fungus *Phomopsis* sp. BCC 1323. Both are xanthone dimers. Xanthones are also included in the polyphenol (flavonoid) group. Although xanthones have a simple chemical structure, they have many chemicals that produce various types of xanthones, such as simple oxygenated xanthones, xanthone glycosides, prenylated and related xanthones, xanthoneolignoids, and other xanthones. Previous research results have proven that xanthones have biological activities such as anticancer, antimicrobial, antimalarial, anticholinesterase, anti-HIV, anti-inflammatory, anticonvulsant, antioxidant, and cardiovascular. Phomoxanthone is part of xanthone (Ramos *et al.* 2022). These two compounds also have antimalarial activity against *P. falciparum* (K1, a multidrug-resistant strain) and antituberculosis activity against Mycobacterium tuberculosis (strain H37Ra), have cytotoxic activity against KB and BC-1 cancer cells, and Vero cells. In some cases, Phomoxanthone A was more toxic to the test cell lines than Phomoxanthone B. In another study, Phomoxanthone A inhibited the growth of the Gram-positive *Bacillus megaterium*, the alga *Chlorella fusca*, and the fungus *Ustilago* (Böhler *et al.* 2018), and inhibitors of protein tyrosine phosphatase, which can cause all types of cancer, diabetes, and autoimmune diseases (Yang *et al.* 2020). Phomoxanthone A has also been known as an antitumor (Pavão *et al.* 2016) and also as a natural compound with strong apoptotic anticancer effects against platinum-resistant solid cancers (Wang *et al.* 2019). Phomoxanthone A was found to have acetylcholinesterase and glucosidase inhibitory activity, antimicrobial, and antioxidant (Zhu *et al.* 2023). Phomoxanthone A, produced from Phomopsis longicolla has antitumor/anticancer properties. Previous research results also showed that Phomoxanthone A has strong activity against ovarian and bladder cancer cells. Phomoxanthone A is a natural compound with strong anticancer apoptotic effects against platinum-resistant solid cancers (Wang *et al.* 2019). Phomoxanthone A is also known as an immunostimulant to increase antibodies for immunity and ward off pathogens that enter the body (Woods *et al.* 2017).

Phomoxanthone B and derivatives also have antimicrobial activity (Eshboev *et al.* 2024). Other studies also state that Phomoxanthone can be isolated from the fungus Phomopsis sp xy21, and six dimers, named Phomoxanthone F to K, were obtained. Among the six dimers, only Phomoxanthone F has a weak anti-HIV effect (Hu *et al.* 2018).

In this study, Phomoxanthone was detected in UV at 235 nm, but in previous studies, Phomoxanthone was detected at max 212 nm, 258 nm, and 336 nm. However, in the results of this study, Phomoxanthone detected in UV 235 nm was still in the Phomoxanthone range (212 -336 nm). As seen in the DAD UV-Vis results. In the LC-MS results using HPLC-DAD MS for molecular weight analysis, no Phomoxanthone compounds were detected or identified. Phomoxanthone is known to have 8 dimers, namely Phomoxanthone A-H. Based on a literature review of Phomoxanthone compounds, the molecular weight

of the 8 Phomoxanthones is between 276.44-750.7 g/mol. The highest molecular weight range of 750.7 g/mol is owned by Phomoxanthone A and Phomoxanthone B. This molecular range is not detected on the mass spectrometer (MS). The molecular weight range that is close to Phomoxanthone A and B, which is 783.3 g/mol detected on LC-MS, is not the molecular weight of Phomoxanthone A (750.70 g/mol) or Phomoxanthone B (750.74 g/mol). These results are evidenced by the retention time of the Phomoxanthone compound detected on UV-Vis DAD, which is in the retention time range of 7,670-17.5 minutes, different from the molecular weight of 783.3 g/mol detected on LC-MS with a retention time of 19.37-19.66 minutes. So, this data proves that the molecular weight of 783.3 g/mol detected on LC-MS is not the molecular weight of Phomoxanthone A or B. The molecular weight of Phomoxanthone cannot be detected on LC-MS because the specifications of the HPLC DAD MS tool cannot detect Phomoxanthone. The use of the HPLC DAD MS tool to analyze molecular weight cannot detect Phomoxanthone because LC-MS on the use of the HPLC DAD MS tool can analyze more widely compounds that are thermally labile, high polarity or high molecular mass and even high molecular proteins. The weakness is that it cannot detect volatile (easily evaporated) compounds or low polarity or molecular mass. That is why in the LC-MS analysis, Phomoxanthone with a smaller molecular mass cannot be detected on LC-MS. This is reinforced by the retention time of Phomoxanthone on UV-Vis DAD, which is the smallest among other compounds. A smaller retention time indicates that the compound is easily ionized (separated) based on polarity and speed of reaching the detector. That is why in UV-Vis with a DAD detector, Phomoxanthone was detected first with the fastest retention time (indicated by a smaller retention time value) to the detector so that it can be read. That is why Phomoxanthone was not detected in LC-MS. However, in terms of molecular weight, it is not too far from the molecular weight of the compound 783.3 g/mol which was read on the detector. When compared to the molecular weight of 783.3 g/mol detected in LC-MS, Phomoxanthone has a smaller polarity, so it is easily separated with a faster movement speed in the column through the stationary phase and is volatile so that in an LC-MS, it cannot be detected by the detector. Although Phomoxanthone was not detected in LC-MS, with UV-Vis DAD, the presence of Phomoxanthone in the most active fraction (F7) of H. aculeatus leaves can be detected. Therefore, the presence of Phomoxanthone detected in the active fraction (F7) of *H. aculeatus* leaves is an antiplasmodial compound. This is supported by previous studies that state that Phomoxanthone is known as an antimalarial that can cure malaria caused by the *Plasmodium parasite* (Böhler *et al.* 2018; Yang *et al.* 2020).

Cyclopenin detected at UV 235 nm in previous studies had little antibacterial activity against Pyogenem var Micrococcus aureus and Escherichia coli. Cyclopenin was first isolated from *Penicillium cyclopium* culture filtrate with a molecular weight of 294.31 $g.mol^{-1}$. Based on the results of the analysis by LC-MS (Table. 9), no molecular weight similar to cyclopenin was detected. Cyclopenin has also been isolated from the bacteria Brevibacterium halotolerans, which acts as an antagonist to inhibit the growth of bacterial and fungal pathogens in apple plants (Ahmed *et al.* 2015). In addition, it was also isolated from the fungus P. crustosum (Antipova *et al.* 2018) and has antibacterial activity (Feng *et al.* 2021). It was also isolated from Penicillium solitum (Boruta *et al.* 2018). Cyclopenin isolated from *Penicillium polonicum* MCCC3A00951 has inhibitory activity against influenza (Liu *et al.* 2020b). Cyclopenin is also known to have antibacterial activity against *E. coli* (Pan *et al.* 2016). Cyclopenin isolated from the extract of *Aspergillus* sp. SCSIOW2 strain fungus in the sea has antioxidant and anti-inflammatory activities, especially in improving brain inflammation due to Alzheimer's disease (Lu *et al.* 2020). Cyclopenin isolated from the extract of endophytic fungi has antioxidant and immunosuppressive activities (Ujam *et al.* 2021). Cyclopenin is also known as an anti-inflammatory and anti-inflammatory agent for neurodegenerative diseases (Wang *et al.* 2020). Cyclopenin analogs also have potential as Sars-Cov-2 Mpor antivirals (Thissera *et al.* 2021).

Microsphaerone has two dimers, namely microsphaerone A and B. Both have molecular weights of 433.1658 and 319.1420, respectively (NCBI & NIH 2006; Cheng *et al.* 2020). In this study, microsphaerone was detected at UV 235 nm, while the LC/MS results showed that the same molecular weight as the previous study was not found. Microsphaerone is known as a class of flavonoid-pyrones compounds (Song *et al.* 2023). Phytochemical test results with $FeCl_3$ spray reagent proved the presence of phenolic compounds and flavonoids. Microsphaerone has been isolated from an undescribed fungus of the genus Microsphaeropsis, isolated from the Mediterranean sponge *Aplysina aerophoba* (Cheng *et al.* 2020). Microsphaerone is known to have antifungal activity, cell adhesion inhibition activity, and insecticidal activity against Spodoptera littoralis and Artemia salina (Gonzalez-Menendez *et al.* 2017; Song *et al.* 2023).

Indole-3-carbaldehyde is a bioactive metabolite of tryptophan in fungi and bacteria, inducing plant defense responses and resulting particularly abundant in vegetables of the Brassicaceae (Cru-ciferae) family, with a broad therapeutic potential, also acting as a neuroprotective agent, inducing plant defense responses and ensuring the human intestinal barrier integrity (Pappolla *et al.* 2021; Palladino *et al.* 2024). Indole-3-carbaldehyde is a class of indole compounds. Indole is a heterocyclic aromatic organic compound with the formula C_8H_7N. This group of compounds has a bicyclic structure consisting of a six-membered benzene ring fused to a five-membered pyrrole ring. Indole is widely distributed in nature and can be produced by various bacteria. As a molecule that transmits signals between cells, indole regulates various aspects of bacterial physiology, including spore formation, plasmid stability, drug resistance, biofilm formation, and virulence. Indole also functions as an anticancer, anti-leukemic, antiemetic, immunomodulatory, vasodilator, antihypertensive, antidepressant, antidepressant, antipsychotic, sexual disorder, anti-inflammatory, Anti-HIV, Schizophrenia, Anti-Asthmatic, antitubercular (Kumar & Ritika 2020; Bajad *et al.* 2022; Cui *et al.* 2022). Some indole molecules produced by the gut microbiota have biological activities such as neuroprotective and antioxidant properties. Managing the microbiota to increase the production of neuroprotective indoles (e.g., indole propionic acid) may improve brain health during aging. Since then, studies have demonstrated additional properties of Indole, including anti-inflammatory, immunoregulatory, and anti-amyloid aggregation properties (Kumar & Ritika 2020; Liu *et al.* 2020a).

Indole-3-carbaldehyde has previously been shown to inhibit the enzyme tyrosinase. Tyrosinase is a key enzyme for melanin biosynthesis in plants, microorganisms, and mammalian cells. Indole-3-carbaldehyde can also inhibit melanin formation through inhibition of the enzyme tyrosinase. This enzyme catalyzes two reactions: the hydroxylation of monophenols to o-diphenols (monophenolase activity) and the oxidation of o-diphenols to o-quinones (diphenolase activity), which are then polymerized into brown, red, or black pigments. These brown, red, or black pigments are caused by excess melanin production. Many tyrosinase inhibitors have been tested in cosmetics and pharmaceuticals as a way to prevent excessive melanin production in the epidermis of the skin. Melanin formation is also thought to impair the color quality of plant-derived foods and prevent the activation of browning. This has attracted scientists to conduct this research. In addition, tyrosinase is one of the main enzymes in the molting process of insects.

Furthermore, it has been reported that tyrosinase may be central to dopamine neurotoxicity and contribute to neurodegeneration associated with Parkinson's disease. Tyrosinase is also involved in the enzymatic browning of mushrooms, which is responsible for the loss of sensory and nutritional qualities. Indole-3-carbaldehyde activity is an inhibitor that inhibits melanin formation through the inhibition of the tyrosinase enzyme (Baber *et al.* 2023).

High-performance liquid chromatography (HPLC) is the main method used for qualitative and quantitative analysis of chemical compounds in samples, including the indole group. This HPLC method can be coupled with mass spectrometry and NMR (Karanikolopoulou *et al.* 2021). In this study, the analysis of chemical compound components in the active fraction of kapur leaves was carried out qualitatively and quantitatively using TLC, UV-Vis with a DAD detector, and HPLC-MS coupled with a UV detector. The UV-Vis with a DAD detector uses the same principle to measure the amount of light absorbed by a sample. The difference is that the UV- In this study, the analysis of chemical compound components in the active fraction of kapur leaves was carried out qualitatively and quantitatively using TLC, UV-Vis with a DAD detector, and HPLC-MS coupled with a UV detector. The UV-Vis DAD detector uses the same principle to measure the amount of light absorbed by a sample. The difference is that the UV-Vis detector is set to measure a specific part of the spectrum simultaneously, while the DAD can calculate the entire spectrum simultaneously. The detector is set to measure a specific part of the spectrum simultaneously, while the DAD can calculate the entire spectrum simultaneously. This makes the DAD method more efficient and convenient than conventional UV-Vis detection. In this study for analysis, HPLC-DAD MS is a liquid chromatography technique.

HPLC-DAD with UV detector coupled to LC-MS or HPLC-MS, Liquid chromatography-mass spectrometry (high performance) is a similar technique that starts with liquid chromatography. The difference is that the separated sample is then passed through a mass spectrometer, where it is ionized, further separated, and detected based on the mass-to-charge ratio of each ion. This makes LC-MS a more sensitive technique that is capable of detecting components in smaller quantities. The molecular weight of this compound is 145.16 $g.mol^{-1}$. Based on the LC-MS data in this study, the molecular weight of this compound was not detected. Indole-3-carbaldehyde has been known to have acted as a corrosion inhibitor tested on steel so that it can be applied in the industry as an acid-washing solution to etch and remove rust from metal surfaces

(Ashhari & Sarabi 2015). Indole-3-carbaldehyde also has antioxidant activity (Subhan *et al.* 2016). Several indole-3-carbaldehyde derivative compounds can be synthesized and are known to have antibacterial activity (Carrasco *et al.* 2020), anticancer (Haribabu *et al.* 2018), and urease inhibitor against Helicobacter pylori (Kalatuwawege *et al.* 2021). Indole-3-carbaldehyde compounds can also be utilized in the process of tryptanthrin synthesis through Dakin oxidation reactions. Tryptanthrin is known to be useful as an antitumor, antimalarial, antiparasitic, antineoplastic activities, COX-2, 5-LOX inhibitors, and PGE expression, rheumatoid arthritis (Onambele *et al.* 2015; Kirpotina *et al.* 2020; Zou *et al.* 2023). Several other indole derivatives have been known to be useful as anticancer, antimalarial, antitubercular, anti-HIV agents, anticonvulsants for the treatment of epilepsy, antimicrobial, anti-diabetic, antiviral (besides HIV, herpes virus, hepatitis B and C), anti-inflammatory, antidepressant, antioxidant, anticholinergic, and antihistamines (Kumari & Singh 2019).

Naamine is a group of alkaloids that have been known to have activity against plant viruses and phytopathogenic fungi (Guo *et al.* 2018). Naamine J, a derivative of naamine, was also found to have mild cytotoxic activity against MCF-7, A549, HeLa, and PC9 cancer cells with IC_{50} values in the range of 20.1-45.3 M (Murniasih *et al.* 2021; Tang *et al.* 2017). Naamine can be isolated from marine sponges and is known to have antimicrobial, antialgacidal, and antifungal activities (Bjørsvik & Sandtorv 2014; Pokharkar *et al.* 2022). Naamine derivatives also have antitumor/anticancer and antimicrobial activities. Naamine also has antifungal activity in plants. Other studies have also stated that naamine derivatives have antifungal and antiviral properties against tobacco mosaic viruses and fungicides (Guo *et al.* 2018; Murniasih *et al.* 2021). Based on data from five compounds identified using UV-Vis DAD, especially at a wavelength of 235 nm, it can be said that these compounds play a major role in supporting antiplasmodial activity in the active fraction (F7) of *H. aculeatus* leaves. This is in line with the IC_{50} and ED_{50} values of FA in the antiplasmodial activity test, which are categorized as very active. Although several other compounds have not been identified, these five compounds are strongly suspected of supporting F7, together with compounds that have not been identified as inhibiting the growth of *P. falciparum*.

The active fraction (F7) of *H. aculeatus* leaves was proven to be selective (with a selectivity index value of 8159.94) in inhibiting/killing Plasmodium both *in vitro* and *in vivo* with an IC_{50} value of 0.7 $g.mL^{-1}$ and an ED_{50} of 2.49 $mg.kg\ BW^{-1}.d^{-1}$. Five compounds identified using UV-Vis have been confirmed according to phytochemical screening and have pharmacological effects, including antiplasmodial. The five compounds identified are phomoxanthone, cyclopenin, microsphaerone, indole-3-carbaldehyde, and Naamine, in addition to 7 compounds that have not been identified.

Acknowledgements

Thank you to the Ministry of Education, Culture, Research, and Technology of the Republic of Indonesia for providing me with a scholarship to complete my doctoral studies at Universitas Gadjah Mada, Yogyakarta. We also thank Universitas Gadjah Mada for providing financial assistance for this Final Project research. I also thank Prof. Dr. Peter Proksch and Dr. Rini Muharini from Heinrich Heine Universitaet, Düsseldorf, Germany, who have helped me analyze samples using the UV-Vis DAD and HPLC-DAD with UV detector tools in Germany. Thank you also to Mr. Rumbi, Mr. Purwono, Mr. Mosa, Mr. Wagimin, and Laboratory Assistants at the Faculty of Medicine, Public Health, and Nursing; Faculty of Pharmacy UGM, and all parties that I cannot mention one by one who has helped me during this research. May the Holy God repay your kindness.

References

Ahmed, H.A., Ebrahim, W., Mikhailovna, P.A., Henrich, B., Proksch, P., 2015. Extraction and identification of some metabolites produced by antagonistic apple plant bacteria *Brevibacterium halotolerans*. *International Journal of Advanced Research*. 3, 1208-1217.

Antipova, T.V., Zhelifonova, V.P., Baskunov, B.P., Kochkina, G.A., Ozerskaya, S.M., Kozlovskii, A.G., 2018. Exometabolites the Penicillium fungi isolated from various high-latitude ecosystems. *Microbiology (Russian Federation)*. 87, 642-651. https://doi.org/10.1134/S002626171805003X

Ashhari, S., Sarabi, A.A., 2015. Indole-3-carbaldehyde and 2-methylindole as corrosion inhibitors of mild steel during pickling. *Pigment and Resin Technology*. 44, 322-329. https://doi.org/10.1108/PRT-11-2014-0104

Baber, M.A., Crist, C.M., Devolve, N.L., Patrone, J.D., 2023. Tyrosinase inhibitors: a perspective. Molecules. 28, 5762. https://doi.org/10.3390/molecules28155762

Bajad, N.G., Singh, S.K., Singh, S.K., Singh, T.D., Singh, M., 2022. Indole: a promising scaffold for the discovery and development of potential antitubercular agents. *Current Research in Pharmacology and Drug Discovery*, 3, 100119. https://doi.org/10.1016/j.crphar.2022.100119

Bjørsvik, H.R., Sandtorv, A., 2014. Synthesis of imidazole alkaloids originated in marine sponges. *Studies in Natural Products Chemistry*. 42, 33-57. https://doi.org/10.1016/B978-0-444-63281-4.00002-1

Böhler, P., Stuhldreier, F., Anand, R., Kondadi, A. K., Schlütermann, D., Berleth, N., Deitersen, J., Wallot-Hieke, N., Wu, W., Frank, M., Niemann, H., Wesbuer, E., Barbian, A., Luyten, T., Parys, J.B., Weidtkamp-Peters, S., Borchardt, A., Reichert, A. S., Peña-Blanco, A., … Stork, B., 2018. The mycotoxin phomoxanthone A disturbs the form and function of the inner mitochondrial membrane. *Cell Death and Disease*. 9, https://doi.org/10.1038/s41419-018-0312-8

Boruta, T., Przerywacz, P., Ryngajllo, M., Bizukojc, M., 2018. Bioprocess-related, morphological, and bioinformatic perspectives on the biosynthesis of secondary metabolites produced by *Penicillium solitum. Process Biochemistry*. 68, 12-21. https://doi.org/10.1016/j.procbio.2018.02.023

Carrasco, F., Hernández, W., Chupayo, O., Álvarez, C. ., Oramas-Royo, S., Spodine, E., Tamariz-Angeles, C., Olivera-Gonzales, P., Dávalos, J., 2020. Indole-3-carbaldehyde semicarbazone derivatives: synthesis, characterization, and antibacterial activities. *Journal of Chemistry*. 2020, 1-9. https://doi.org/10.1155/2020/7157281

Cheng, M.M., Tang, X.L., Sun, Y.T., Song, D.Y., Cheng, Y.J., Liu, H., Li, P.L., Li, G.Q., 2020. Biological and chemical diversity of marine sponge-derived microorganisms over the last two decades from 1998 to 2017. *Molecules*. 25, 1-71. https://doi.org/10.3390/molecules25040853

Cui, B., Chen, X., Guo, Q., Song, S., Wang, M., Liu, J., Deng, Y., 2022. The cell-cell communication signal indole controls the physiology and interspecies communication of *Acinetobacter baumannii. Microbiology Spectrum,* 10, 1-12. https://doi.org/10.1128/spectrum.01027-22

Darlina, D., Aryanti, Teja, K., Aziz, A., 2016. Aktivitas antimalaria ekstrak *n*-hexana daun artemisia cina galur iradiasi terhadap *Plasmodium berghei* ANKA. *Jurnal Ilmu Kefarmasian Indonesia*. 14, 226-232.

Eshboev, F., Mamadalieva, N., Nazarov, P. A., Hussain, H., Katanaev, V., Egamberdieva, D., Azimova, S., 2024. Antimicrobial action mechanisms of natural compounds isolated from endophytic microorganisms. *Antibiotics.* 13, 271. https://doi.org/10.3390/antibiotics13030271

Feng, J., Fan, L., Dan, F., Da-le, G., Bo, R., Yun, D., 2021. Study on the chemical constituents of *Penicillium crustosum,* an endophytic fungus from *Ophiocordyceps sinensis. Natural Product Research and Development*. 33, 1147-1155. https://doi.org/10.16333/j.1001-6880.2021.7.009

Gonzalez-Menendez, V., Martin, J., Siles, J., Gonzalez-Tejero, M.R., Reyes, F., Platas, G., Tormo, J.R., Genilloud, O., 2017. Biodiversity and chemotaxonomy of Preussia isolates from the Iberian Peninsula. *Mycological Progress*. 16, 713-728. https://doi.org/10.1007/s11557-017-1305-1

Guo, P., Li, G., Liu, Y., Lu, A., Wang, Z., Wang, Q., 2018. Naamines and naamidines as novel agents against a plant virus and phytopathogenic fungi. *Marine Drugs*. 16, 1-19. https://doi.org/10.3390/md16090311

Haribabu, J., Tamizh, M. M., Balachandran, C., Arun, Y., Bhuvanesh, N.S.P., Endo, A., Karvembu, R., 2018. Synthesis, structures, and mechanistic pathways of anticancer activity of palladium(ii) complexes with indole-3-carbaldehyde thiosemicarbazones. *New Journal of Chemistry*. 42, 1-37. https://doi.org/10.1039/C7NJ03743K

Hu, H.B., Luo, Y.F., Wang, P., Wang, W.J., Wu, J., 2018. Xanthone-derived polyketides from the Thai mangrove endophytic fungus *Phomopsis* sp. xy21. *Fitoterapia*. 131, 265-271. https://doi.org/10.1016/j.fitote.2018.11.004

Kalatuwawege, I.P., Gunaratna, M.J., Udukala, D.N., 2021. Synthesis, *in silico* studies, and evaluation of syn and anti isomers of n-substituted indole-3-carbaldehyde oxime derivatives as urease inhibitors against helicobacter pylori. *Molecules*. 26, 1-14. https://doi.org/10.3390/molecules26216658

Karanikolopoulou, S., Revelou, P.K., Xagoraris, M., Kokotou, M.G., Constantinou-Kokotou, V., 2021. Current methods for the extraction and analysis of isothiocyanates and indoles in cruciferous vegetables. *Analytica*. 2, 93-120. https://doi.org/10.3390/analytica2040011

Kirpotina, L.N., Schepetkin, I.A., Hammaker, D., Kuhs, A., Khlebnikov, A.I., Quinn, M.T., 2020. Therapeutic effects of Tryptanthrin and Tryptanthrin-6-Oxime in models of Rheumatoid Arthritis. *Frontiers in Pharmacology*. 11, 1-17. https://doi.org/10.3389/fphar.2020.01145

Kumar, S., Ritika, 2020. A brief review of the biological potential of indole derivatives. *Future Journal of Pharmaceutical Sciences.* 6, 121. https://doi.org/10.1186/s43094-020-00141-y

Kumari, A., Singh, R.K., 2019. Medicinal chemistry of indole derivatives: current to future therapeutic prospectives. *Bioorganic Chemistry.* 89, 103021. https://doi.org/10.1016/j.bioorg.2019.103021

Liu, J., Matuszewska, M., Gaimster, H., Summers, D.K., 2020a. Local and universal action: the paradoxes of indole signalling in bacteria. *Trends in Microbiology*. 28, 1-12. https://doi.org/10.1016/j.tim.2020.02.007

Liu, S.Z., He, F.M., Bin, Y. lin, Li, C.F., Xie, B.Y., Tang, X.X., Qiu, Y.K., 2020b. Bioactive compounds derived from the marine-derived fungus MCCC3A00951 and their influenza neuraminidase inhibition activity *in vitro* and *in silico. Natural Product Research*. 35, 5621-5628. https://doi.org/10.1080/14786419.2020.1817015

Lu, X., He, J., Wu, Y., Li, X., Ju, J., Hu, Z., Umezawa, K., Wang, L., 2020. Isolation and characterization of new anti-inflammatory and antioxidant components from deep marine-derived fungus *Myrothecium* sp. Bzo-l062. *Mar. Drugs.* 18, 1-10. https://doi.org/10.3390/md18120597

Muñoz, V., Sauvain, M., Bourdy, G., Callapa, J., Rojas, I., Vargas, L., Tae, A., Deharo, E., 2000. The search for natural bioactive compounds through a multidisciplinary approach in Bolivia. Part II. Antimalarial activity of some plants used by Mosetene indians. *Journal of Ethnopharmacology.* 69, 139-155. https://doi.org/10.1016/S0378-8741(99)00096-3

Murniasih, T., Putra, M.Y., Bayu, A., Wibowo, J.T., 2021 . A review on diversity of anticancer compounds derived from Indonesian marine sponges a review on diversity of anticancer compounds derived from Indonesian marine sponges. *IOP Conf. Ser.: Mater. Sci. Eng.* 1192, 012012. https://doi.org/10.1088/1757-899X/1192/1/012012

NCBI, NIH, 2006. Microsphaerone A. NMRShiftDB. External ID 2581. Categpry Reasearh and Development. Available at https://pubchem.ncbi.nlm.nih.gov/compound/636775. [Date accessed: 9 March 2025]

Onambele, L.A., Riepl, H., Fischer, R., Pradel, G., Prokop, A., Aminake, M.N., 2015. Synthesis and evaluation of the antiplasmodial activity of tryptanthrin derivatives. *International Journal for Parasitology: Drugs and Drug Resistance*. 5, 48-57. https://doi.org/10.1016/j.ijpddr.2015.03.002

Palladino, P., Attanasio, L., Scarano, S., Degano, I., Minunni, M., 2024. Colorimetric determination of indole-3-carbaldehyde by reaction with carbidopa and formation of aldazine in ethanolic extract of cabbage. *Food Chemistry Advances*. 4, 100643. https://doi.org/10.1016/j.focha.2024.100643

Pan, C., Shi, Y., Chen, X., Chen, C.T. ., Tao, X., Wu, B., 2016. New compounds from a hydrothermal vent crab-associated fungus *Aspergillus versicolor* XZ-4. *Organic and Biomolecular Chemistry*. 15, 1155-1163. https://doi.org/10.1039/C6OB02374F

Pappolla, M.A., Perry, G., Fang, X., Zagorski, M., Sambamurti, K., 2021. Neurobiology of disease indoles as essential mediators in the gut-brain axis. Their role in Alzheimer's disease. *Neurobiology of Disease*. 156, 105403. https://doi.org/10.1016/j.nbd.2021.105403

Pavão, G.B., Venâncio, V.P., de Oliveira, A.L.L., Hernandes, L.C., Almeida, M.R., Antunes, L.M.G., Debonsi, H.M., 2016. Differential genotoxicity and cytotoxicity of phomoxanthone A isolated from the fungus *Phomopsis longicolla* in HL60 cells and peripheral blood lymphocytes. *Toxicology in Vitro*. 37, 211-217. https://doi.org/10.1016/j.tiv.2016.08.010

Pokharkar, O., Lakshmanan, H., Zyryanov, G., Tsurkan, M., 2022. *In silico* evaluation of antifungal compounds from marine. *Mar. Drugs*. 20, 215. https://doi.org/10.3390/md20030215

Ramos, G. da C., Silva-Silva, J.V., Watanabe, L.A., Siqueira, J.E., de S., Almeida-Souza, F., Calabrese, K.S., Marinho, A. M. do R., Marinho, P.S.B., Oliveira, A.S.de., 2022. Phomoxanthone A, compound of endophytic fungi *Paecilomyces* sp. and its potential antimicrobial and antiparasitic. *Antibiotics*. 11, 1332. https://doi.org/10.3390/antibiotics11101332

Song, G., Zhang, Z., Niu, X., Zhu, D., 2023. Secondary metabolites from Fungi *Microsphaeropsis* spp.: chemistry and bioactivities. *J. Fungi.* 9, 1093. https://doi.org/10.3390/jof9111093

Subhan, H., Ahmad, K., Lashin, A., Rana, U., Abbasi, R., Hussain, H., Mahmood, A., Qureshi, R., Kraatz, H.B., Shah, A., 2016. pH and temperature responsive electrooxidation and antioxidant activity of indole-3-carbaldehyde. *Journal of The Electrochemical Society*. 163, 690-696. https://doi.org/10.1149/2.0931608jes

Tang, W.Z., Yang, Z., Sun, F., Wang, S.P., Yang, F., Lin, H.W., 2017. Leucanone A and naamine J, glycerol ether lipid and imidazole alkaloid from the marine sponge *Leucandra* sp. *Journal of Asian Natural Products Research*. 19, 691-696. https://doi.org/10.1080/10286020.2016.1240171

Thissera, B., Sayed, A., Hassan, H.A., Abdelwahab, F., Amaeze, N., Semler, T., Alenezi, F.N., Yaseen, M., Alhadrami, H.A., Belbahri, L., Rateb, M.E., 2021. Bioguided isolation of cyclopenin analogues as potential sars-cov-2 mpro inhibitors from *Penicillium citrinum* tdpef34. *Biomolecules*. 11, 1-12. https://doi.org/10.3390/biom11091366

Trager, W., Jensen, J., 1976. Human malaria parasites in continuous culture. *Science*. 193, 673-675. https://doi.org/10.1126/science.781840

Turalely, R. (2018). Antiplasmodial activity test of fraction 12 (FG12) methanol extract of Kapur leaf (*Harmsiopanax aculeatus* Harms). *Molluca Journal of Chemistry Education.* 8, 71-75.

Turalely, R., Mustofa, Hertiani, T., Wijayanti, M.A., 2022. Active compounds of Kapur plant (*Harmsiopanax aculeatus*) from Maluku: study of antiplasmodial activity and characterization of active compounds structure. *Heliyon.* 1-14. https://doi.org/10.2139/ssrn.4171586

Turalely, R., Mustofa, M., Wijayanti, M.A., Hertiani, T., 2018. Activity of anti-plasmodial and cytotoxicity of Kapur leaves (*Harmsiopanax aculeatus*, Harms) potential fraction (FG2, FG3, and FG4) traditionally used to treat malaria in Maluku Indonesia. *Jurnal Kimia dan Pendidikan Kimia*. 3, 46.https://doi.org/10.20961/jkpk.v3i2.21068

Turalely, R., Susidarti, R.A., Wijayanti, M.A., 2011. *In vivo* antiplasmodial of the most active fraction and its compound of Kapur leaves (*Harmsiopanax aculeatus* Harms) extract against *Plasmodium berghei. Tropical Medicine Journal*. 1, 131-140. https://doi.org/https://doi.org/10.22146/tmj.4575

Turalely, R., Wijayanti, M.A., Hertiani, T., Mustofa., 2020a. Antiplasmodial activity and cytotoxicity of kapur (*Harmsiopanax aculeatus*) leaf extracts traditionally used for the treatment of malaria in Maluku. *Indonesian Journal of Pharmacology and Therapy*. 1, 22-30. https://doi.org/10.22146/ijpther.512

Turalely, R., Wijayanti, M.A., Hertiani, T., Mustofa, 2020b. *In vitro* antiplasmodial activity and cytotoxicity of active subfractions of *Harmsiopanax aculeatus* leaves. *Indonesian Journal of Pharmacy*. 31, 51-55. https://doi.org/10.14499/indonesianjpharm31iss1pp51

Ujam, N.T., Ajaghaku, D.L., Okoye, F.B.C., Esimone, C.O., 2021. Antioxidant and immunosuppressive activities of extracts of endophytic fungi isolated from *Psidium guajava* and *Newbouldia laevis. Phytomedicine Plus*. 1, 1-7. https://doi.org/10.1016/j.phyplu.2021.100028

Wang, C., Engelke, L., Bickel, D., Hamacher, A., Frank, M., Proksch, P., Gohlke, H., Kassack, M.U., 2019. The tetrahydroxanthone-dimer phomoxanthone A is a strong inducer of apoptosis in cisplatin-resistant solid cancer cells. *Bioorganic and Medicinal Chemistry*. 27, 115044. https://doi.org/10.1016/j.bmc.2019.115044

Wang, L., Li, M., Lin, Y., Du, S., Liu, Z., Ju, J., Suzuki, H., Sawada, M., Umezawa, K., 2020. Inhibition of cellular inflammatory mediator production and amelioration of learning deficit in flies by deep sea Aspergillus-derived cyclopenin. *Journal of Antibiotics*. 73, 622-629. https://doi.org/10.1038/s41429-020-0302-9

Woods, N., Niwasabutra, K., Acevedo, R., Igoli, J., Altwaijry, N.A., Tusiimire, J., Gray, A.I., Watson, D.G., Ferro, V.A., 2017. Natural vaccine adjuvants and immunopotentiators derived from plants, fungi, marine organisms, and insects. In: Schijns VEJC, O'Hagan DT (Eds.). *Immunopotentiators in Modern Vaccines: Second Edition.* Amsterdam: Academic Press. pp. 211-229. https://doi.org/10.1016/B978-0-12-804019-5.00011-6

Yang, R., Dong, Q., Xu, H., Gao, X. H., Zhao, Z., Qin, J., Chen, C., Luo, D., 2020. Identification of phomoxanthone A and B as protein tyrosine phosphatase inhibitors. *ACS Omega*. 5, 25927-25935. https://doi.org/10.1021/acsomega.0c03315

Zhu, J., Wang, Z., Song, L., Fu, W., Liu, L., 2023. Anti-alzheimer's natural products derived from plant endophytic fungi. *Molecules*. 28, 2259. https://doi.org/10.3390/molecules28052259

Zou, Y., Zhang, G., Li, C., Long, H., Chen, D., Li, Z., Ouyang, G., Zhang, W., Zhang, Y., Wang, Z., 2023. Discovery of tryptanthrin and its serivatives and its activities against NSCLC *in vitro* via both apoptosis and autophagy pathways. *International Journal of Molecular Sciences*. 24, 1450. https://doi.org/10.3390/ijms24021450